Polyhedron 81 (2014) 499–510

Contents lists available at ScienceDirect

Polyhedron

journal homepage: www.elsevier.com/locate/poly

Sterically modulated palladium(II)–*N*-heterocyclic carbene complexes for the catalytic oxidation of olefins: Synthesis, crystal structure, characterization and DFT studies

Abbas Washeel Salman [a,c], Ghani Ur Rehman [b], Norbani Abdullah [c,*], Srinivasa Budagumpi [d], Salasiah Endud [b,*], Hassan Hadi Abdallah [e], Wen Yee Wong [b]

[a] Department of Chemistry, College of Science, Wasit University, Kut, Wasit, Iraq
[b] Department of Chemistry, Faculty of Science, Universiti Teknologi Malaysia, 81310 UTM Johor Bahru, Johor, Malaysia
[c] Department of Chemistry, Faculty of Science, University of Malaya, 50603 Kuala Lumpur, Malaysia
[d] Centre for Nano and Material Sciences, Jain University, Jain Global Campus, Bangalore 562 112, Karnataka, India
[e] Department of Chemistry, Education College, Salahaddin University, Erbil, Iraq

ARTICLE INFO

Article history:
Received 30 April 2014
Accepted 18 June 2014
Available online 5 July 2014

Keywords:
1-Octene
DFT study
Olefin epoxidation
Palladium(II)-carbene complex
X-ray diffraction

ABSTRACT

The synthesis of a series of sterically modulated palladium(II)–NHC complexes (**9**–**11**) of the general formula $[Pd(NHC)_2Cl_2]$ (NHC = 1-benzyl-3(2′-methyl)-propylbenzimidazol-2-ylidine, 1-benzyl-3(2′-methyl)-butylbenzimidazol-2-ylidine and 1-benzyl-3-hexylbenzimidazol-2-ylidine) from their respective silver(I) counterparts (**6**–**8**) is presented. Two novel triazine-tethered Zwitterionic (benz)imidazolium salts, **4** and **5**, were prepared and tested as NHC precursors for the preparation of silver(I) complexes. However, all our attempts to prepare silver(I) derivatives from salts **4** and **5** ended with negative results due to the low acidity of the C2 protons. The Zwitterionic derivative **4** was additionally characterized by the single crystal X-ray diffraction technique. The molecular structure of **4** evidenced π–π stacking interactions between the triazine rings of two crystallographically independent units. The palladium complexes **9**–**11** showed good catalytic activities in the epoxidation of 1-octene and styrene under homogeneous conditions with aqueous hydrogen peroxide as an oxidant. The effect of temperature and solvent on the epoxidation of the aforementioned olefins using complexes **9**–**11** was also explored. Density functional theory (DFT) was used to model the structures of the isomers of the palladium complexes. Geometry parameters, electronic energy, molecular orbital energies, band gap, vibrational frequencies and the cis–trans energy barrier were calculated.

1. Introduction

The field of N-heterocyclic carbene (NHC) chemistry has undergone an incredible expansion ever since its discovery more than half a century ago. Recent investigations have focused on understanding the mode of interactions of NHC ligands with both transition and inner transition metals in various oxidation states [1]. Interestingly, these outcomes shed light on the complexation behavior of multidentate NHC systems containing three or more coordination donor sites to address key factors influencing complex formation. The second row congeners of group 10 and 11, palladium and silver, present a unique combination for both bioorganometallic chemistry and catalysis from isostructural complexes having NHC ligands. Silver(I)–NHC complexes have been active as anticancer [2] and antibacterial agents due to their favorable biocompatible properties [3], while palladium(II)–NHC complexes have been studied for numerous C–C, C–N coupling and cross-coupling [4] and C–H activation [5] reactions (Chart 1). In particular, organometallic palladium(II)–NHC complexes, popularized by many research groups, have gained considerable attention in recent years due to their facile preparation through NHC transfer from silver(I) counterparts *via* a transmetallation technique [6]. A number of recent studies have targeted the polymerization of olefins with these molecules [7] and their heterogeneous counterparts [8].

Mono- and bidentate NHC systems derived from imidazolium and benzimidazolium derivatives provide a square-planar coordination sphere for palladium(II)–NHC complexes and generally they posses increased stability towards air and moisture. A plethora of

* Corresponding authors. Tel.: +60 3 7967 4264 (N. Abdullah). Tel.: +60 1 97311635; fax: +60 7 5566162 (S. Endud).
E-mail addresses: norbania@um.edu.my (N. Abdullah), salasiah@kimia.fs.utm.my (S. Endud).

http://dx.doi.org/10.1016/j.poly.2014.06.054
0277-5387/

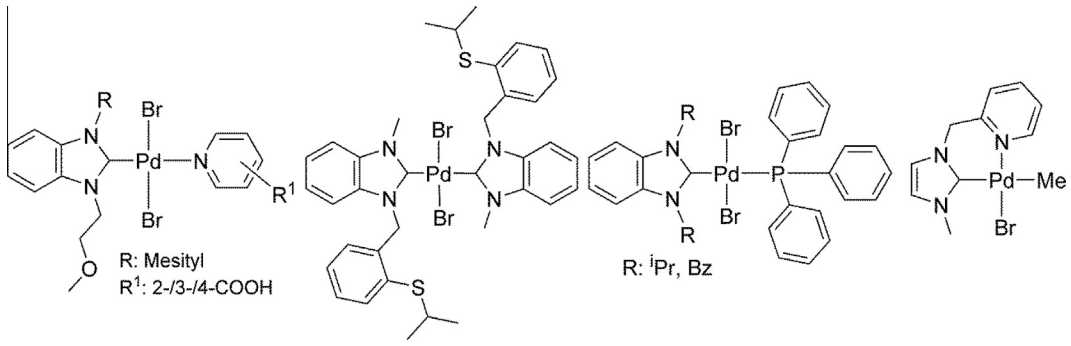

Chart 1. Benzimidazole-derived Pd(II)–NHC complexes.

these complexes are used for various C–C and C–N bond formation reactions, however their potential in olefin epoxidations is very rarely reported. On the other hand, the use of hydrogen peroxide, one of the greenest terminal oxidants, for the epoxidation of olefins in connection with palladium(II)–NHC complexes is of great interest due to the importance of epoxides as well as other oxidized products in the manufacture of both bulk and fine chemicals [9]. A large portion of these catalyses have involved group 7 to 9 metals with numerous multidentate N-donor and N,O-donor ligands [10]. A key point in the production of epoxides or other desired oxidized products from olefins is the activation of catalyst species in the absence or at very low concentrations of oxidants. With this perspective, new oxidative processes based on the activation of hydrogen peroxide by stable, proficient and highly selective catalysts were developed [11].

In view of ever increasing environmental awareness, imidazole-based acetamide/group 7 systems and their counterparts have been reported as homogeneous and heterogeneous catalysts for olefin epoxidation with hydrogen peroxide as a terminal oxidant. Special attention was recently devoted to the use of group 10 metal complexes for this application, which are more specific and robust compared to group 7 systems [12]. These types of complex systems show considerable catalytic activities under different reaction conditions [13]. The efficiency of these homogeneous catalysts and their heterogeneous counterparts in olefin epoxidations led us to design the present NHC complexes. Starting from these results and the efficient catalytic applications of palladium(II)–NHC complexes, an investigation of the steric influence on olefin epoxidation is presented in the present manuscript. We investigate here the synthesis, characterization and DFT studies of a series of new palladium(II)–NHC complexes prepared *via* the transmetallation method from silver(I)–NHC complexes. Further, we described the efficient and selective epoxidation of 1-octene and styrene with 30% aqueous hydrogen peroxide in the presence of palladium(II)–NHC complexes as homogenous solid catalysts.

2. Experimental

2.1. Reagents and instruments

All the chemicals used were of reagent grade, and the solvents were dried and distilled before use according to the standard procedures. Benzyl bromide, benzimidazole, imidazole, cyanuric chloride, 2-methylpropyl bromide, 2-methylbutyl bromide, n-hexyl bromide, silver(I) oxide, palladium(II) chloride, 1-octene, styrene and 30% aqueous hydrogen peroxide were purchased from Sigma–Aldrich and used as received. 1-Benzylbenzimidazole, 1-butylimidazole and 1-butylbenzimidazole were synthesized according to a literature procedure with minor modifications [14]. ^{1}H and ^{13}C NMR spectra of all the compounds were recorded at room temperature on a Bruker 500 MHz Ascend spectrometer in DMSO-d_6 or D_2O solvent using TMS as an internal reference. The FTIR spectra of all the compounds were recorded in potassium bromide disks using a Perkin Elmer 2000 system spectrometer in the range 4000–400 cm^{-1}. The melting points were assessed using a Stuart Scientific SMP-1 (UK) instrument. All reported compounds were analyzed for carbon, hydrogen and nitrogen by CHN microanalyses using a Perkin Elmer 2400 LS Series CHN/S analyzer. For single crystal X-ray diffraction analysis, a Bruker SMART APEX2-2009 CCD area detector diffractometer was used for the data collection. SAINT Bruker-2009 was used for the cell refinement, SAINT was used for the data reduction and SHELXTL was used to solve the structure. Calculations, structure refinement, molecular graphics and the material for publication were obtained using the SHELXTL and PLATON software packages. The structures were solved by direct methods and refined by full-matrix least-squares against F_2. All non-hydrogen atoms were refined anisotropically. The hydrogen atoms were fixed at calculated positions and refined using a riding mode. The oxidized products of the olefins were analyzed by a Hewlett–Packard 6890N gas chromatograph using an Ultra-1 column and a Hewlett–Packard GC-MSD instrument using an HP5 column.

2.2. Syntheses

2.2.1. Synthesis of 1-benzyl-3-(2′-methyl)propylbenzimidazolium-bromide (**1**)

In a 100 mL round-bottom flask, 1-benzylbenzimidazole (0.208 g, 1.0 mmol) was dissolved in acetonitrile (20 mL) and 2-methylpropyl bromide (0.164 g, 1.2 mmol) was added while stirring. The reaction mixture was brought to reflux and stirred for 48 h. The solvent was removed in vacuo, leaving a beige solid which was washed with diethyl ether (3 × 5 mL) and dried. Yield: 78.4%. M.P.: 143–143.5 °C. ^{1}H NMR (500 MHz, d_6-DMSO) δ: 1.12 (6H, d J = 7.0 Hz, $NCH_2CH(CH_3)_2$), 2.16–2.25 (1H, m, NCH_2-$CH(CH_3)_2$), 4.67 (2H, t J = 6.5 Hz,$NCH_2CH(CH_3)_2$), 5.64 (2H, s, benzylic CH_2), 7.23–7.31 (5H, m, benzyl-*H*), 7.76–7.85 (2H, m, benzimidazole-*H*), 8.11–8.18 (2H, m, benzimidazole-*H*), 10.12 (H, s, benzimidazole-*H2′*). ^{13}C{^{1}H} NMR (125 MHz, d_6-DMSO) δ: 13.7 ($NCH_2CH(CH_3)_2$), 21.7 ($NCH_2CH(CH_3)_2$), 50.4 ($NCH_2CH(CH_3)_2$), 52.8 (benzylicCH_2), 118.9, 122.5, 125.3, 133.2 (Ar-*C* benzyl), 117.3, 121.4, 125.6, 133.7, 134.1, (Ar-*C* benzimidazole), 140.2 (benzimidazolium *C2′*). FT-IR (KBr disc) cm^{-1}: 2923, ~2860 ν(C–H), 1612 ν(C=N, benzimidazole), 1101 ν(C–N, benzimidazole). *Anal.* Calc. for $C_{18}H_{21}N_2Br$: C, 62.6; H, 6.1; N, 8.1. Found: C, 62.9; H, 6.0; 8.3%.

2.2.2. Synthesis of 1-benzyl-3-(2′-methyl)butylbenzimidazolium bromide (**2**)

This compound was prepared in a manner analogous to that for **1**, only with 2-methylbutyl bromide (0.18 g, 1.2 mmol) instead of 2-methylpropyl bromide. Yield: 91.1%. M.P.: 121–122 °C. ^{1}H NMR

(500 MHz, d_6-DMSO) δ: 0.91 (6H, d J = 6.5 Hz, $NCH_2CH_2CH(CH_3)_2$), 2.01–2.10 (1H, m, $NCH_2CH_2CH(CH_3)_2$), 3.35 (2H, quart J = 5.5 Hz, $NCH_2CH_2CH(CH_3)_2$), 4.72 (2H, t J = 6.0 Hz,$NCH_2CH_2CH(CH_3)_2$), 5.91 (2H, s, benzylic CH_2), 7.11–7.20 (5H, m, benzyl-*H*), 7.65–7.73 (2H, m, benzimidazole-*H*), 8.0–8.09 (2H, m, benzimidazole-*H*), 9.92 (H, s, benzimidazole-*H2′*). $^{13}C\{^1H\}$ NMR (125 MHz, d_6-DMSO) δ: 12.2 ($NCH_2CH_2CH(CH_3)_2$), 21.7 ($NCH_2CH_2CH(CH_3)_2$), 28.4 ($NCH_2CH_2CH(CH_3)_2$), 51.2 ($NCH_2CH_2CH(CH_3)_2$), 52.7 (benzylicCH_2), 116.6, 118.3, 124.2, 134.7 (Ar-*C* benzyl), 117.5, 122.7, 124.0, 133.5, 135.0, (Ar-*C* benzimidazole), 139.4 (benzimidazolium *C2′*). FT-IR (KBr disc) cm^{-1}: ~2930, 2867 ν(C–H), 1622 ν(C=N, benzimidazole), ~1050 ν(C–N, benzimidazole). *Anal.* Calc. for $C_{19}H_{23}N_2Br$: C, 63.5; H, 6.4; N, 7.8. Found: C, 63.3; H, 6.0; 7.3%.

2.2.3. Synthesis of 1-benzyl-3-hexylbenzimidazolium bromide (**3**)

This compound was prepared in a manner analogous to that for **1**, only with n-hexyl bromide (0.198 g, 1.2 mmol) instead of 2-methylpropyl bromide. Yield: 83.1%. M.P.: 144–145 °C. ^1H NMR (500 MHz, d_6-DMSO) δ: 0.85 (3H, t J = 7.2 Hz, $N(CH_2)_5CH_3$), 1.30–1.40 (2H, m, $N(CH_2)_4CH_2CH_3$), 2.11–2.28 (2H, quart, $N(CH_2)_3CH_2CH_2CH_3$), 2.87–2.95 (2H, quart, $N(CH_2)_2CH_2(CH_2)_2CH_3$), 3.60–3.67 (2H, quart, $NCH_2CH_2(CH_2)_3CH_3$), 4.74 (2H, t J = 6.4 Hz, $NCH_2(CH_2)_4CH_3$), 5.77 (2H, s, benzylic CH_2), 7.16–7.23 (3H, m, benzyl-*H*), 7.30–7.36 (2H, m, benzyl-*H*), 7.65 (2H, t J = 7.2 Hz, benzimidazole-*H*), 8.21–8.30 (2H, m, benzimidazole-*H*), 10.05 (H, s, benzimidazole-*H2′*). $^{13}C\{^1H\}$ NMR (125 MHz, d_6-DMSO) δ: 11.6 ($N(CH_2)_5CH_3$), 19.3 ($N(CH_2)_4CH_2CH_3$), 23.7 ($N(CH_2)_3CH_2CH_2CH_3$), 27.8 ($N(CH_2)_2CH_2(CH_2)_2CH_3$), 35.2 ($NCH_2CH_2(CH_2)_3CH_3$), 51.6 ($NCH_2(CH_2)_4CH_3$), 52.8 (benzylic$CH_2$), 117.6, 119.1, 125.5, 133.4 (Ar-*C* benzyl), 118.7, 123.4, 132.6, 135.3, (Ar-*C* benzimidazole), 137.7 (benzimidazolium *C2′*). FT-IR (KBr disc) cm^{-1}: 2939, ~2870 ν(C–H), 1628 ν(C=N, benzimidazole), 1064 ν(C–N, benzimidazole). *Anal.* Calc. for $C_{20}H_{25}N_2Br$: C, 64.3; H, 6.7; N, 7.5. Found: C, 64.7; H, 6.3; 7.8%.

2.2.4. Synthesis of 4-(3-butyl-2,3-dihydro-imidazol-1-yl)-[1,3,5]triazin-2,4-diol anion (**4**)

1-Butylimidazole (0.124 g, 1 mmol) in 20 mL of dry acetone was placed in a 150 mL round bottom flask connected to N_2 gas and equipped with a stirrer. The flask was immersed in an ice bath and cyanuric chloride (0.183 g, 1 mmol) in 20 mL of dry acetone was added dropwise over 30 min. An off-white precipitate formed after the complete addition. The stirring was continued for another 2 h under the same reaction conditions and then for 4 h at room temperature. The precipitate that formed was collected by filtration, washed with fresh acetone (2 × 5 mL) and dried in a vacuum desiccator. Yield: 68.5%. M.P.: >300 °C. ^1H NMR (500 MHz, D_2O) δ: 0.83 (3H, t, J = 6.2 Hz, $NCH_2CH_2CH_2CH_3$), 1.28–1.37 (2H, m, $NCH_2CH_2CH_2CH_3$), 1.83–1.91 (2H, m, $NCH_2CH_2CH_2CH_3$), 4.33 (4H, t, J = 6.5 Hz, $NCH_2CH_2CH_2CH_3$), 7.58 (2H, d, J = 6.0 Hz, imidazolium *H5′*), 7.97 (2H, d, J = 6.0 Hz, imidazolium *H4′*), 8.91 (2H, s, imidazolium *H2′*). $^{13}C\{^1H\}$ NMR (125 MHz, D_2O) δ: 13.3 ($NCH_2CH_2CH_2CH_3$), 20.2 ($NCH_2CH_2CH_2CH_3$), 30.8 ($NCH_2CH_2CH_2CH_3$), 51.8 ($NCH_2CH_2CH_2CH_3$), 122.2, 124.7 (imidazolium *C5′* and *C4′*), 136.1 (imidazolium *C2′*), 160.3 (cyanuric NCN), 163.1, 164.7 (cyanuric 2 × *C*-O). FT-IR (KBr disc) cm^{-1}: 2933, ~2875 (C–H), ~1615 ($C{=}N_{imid}$), 1628 ($C{=}N_{triazine}$), ~1045, 1083 ($C_{arom}{-}N_{imid}$). *Anal.* Calc. for $C_{10}H_{13}N_5O_2$: C, 51.1; H, 5.6; N, 29.8. Found: C, 50.7; H, 5.6; N, 30.1%.

2.2.5. Synthesis of 4-(3-butyl-2,3-dihydro-benzimidazol-1-yl)-[1,3,5]triazin-2,4-diol anion (**5**)

This compound was prepared in a manner analogous to that for **4**, only with 1-butybenzlimidazole (0.175 g, 1 mmol) instead of 1-butylimidazole. Yield: 72.7%. M.P.: >300 °C. ^1H NMR (500 MHz, D_2O) δ: 0.91 (3H, t, J = 6.6 Hz, $NCH_2CH_2CH_2CH_3$), 1.32–1.39 (2H, m, $NCH_2CH_2CH_2CH_3$), 1.85–1.92 (2H, m, $NCH_2CH_2CH_2CH_3$), 4.76 (4H, t, J = 7.2 Hz, $NCH_2CH_2CH_2CH_3$), 7.32 (3H, t J = 5.5 Hz, benzimidazolium-*H*), 7.73 (2H, d J = 6.0 Hz, benzimidazolium-*H*), 8.23–8.30 (5H, m, benzyl-*H*), 9.01 (2H, s, benzimidazolium *H2′*). $^{13}C\{^1H\}$ NMR (125 MHz, D_2O) δ: 11.8 ($NCH_2CH_2CH_2CH_3$), 21.0 ($NCH_2CH_2CH_2CH_3$), 33.5 ($NCH_2CH_2CH_2CH_3$), 50.6 ($NCH_2CH_2CH_2CH_3$), 116.3, 123.2, 127.0, 133.0 (Ar-*C* benzimidazole), 137.3 (benzimidazolium *C2′*), 162.0 (cyanuric NCN), 164.4, 164.9 (cyanuric 2 × *C*-O). FT-IR (KBr disc) cm^{-1}: ~2950, ~2830 (C–H), 1613 ($C{=}N_{benzimid}$), 1621 ($C{=}N_{triazine}$), 1034, ~1080 ($C_{arom}{-}N_{benzimid}$). *Anal.* Calc. for $C_{14}H_{15}N_5O_2$: C, 58.9; H, 5.3; N, 24.5. Found: C, 59.3; H, 5.6; N, 24.1%.

2.2.6. Synthesis of bis-[1-benzyl-3-(2′-methyl)propylbenzimidazolium] silver(I) bromide (**6**)

To a stirred solution of the benzimidazolium salt **1** (0.347 g, 1 mmol) in methanol (25 mL) was added silver(I) oxide (0.126 g, 0.055 mmol) in a 50 mL round-bottom flask. The reaction mixture was allowed to stir at room temperature for 48 h in the dark, after which the reaction mixture was filtered through a bed of Celite to remove unreacted silver(I) oxide. The solvent was then removed in vacuo, leaving a colorless solid which was washed with diethyl ether (3 × 5 mL) and recrystallized from methanol/diethyl ether. Yield: 52.1%. M.P.: 223–224 °C. ^1H NMR (500 MHz, d_6-DMSO) δ: 0.97 (12H, d J = 7.2 Hz, 2 × $NCH_2CH(CH_3)_2$), 1.96–2.05 (2H, m, 2 × $NCH_2CH(CH_3)_2$), 4.43 (4H, t J = 6.8 Hz,2 × $NCH_2CH(CH_3)_2$), 5.38 (4H, s, benzylic CH_2), 7.20–7.28 (10H, m, benzyl-*H*), 7.50–7.58 (4H, m, benzimidazole-*H*), 7.91–8.01 (4H, m, benzimidazole-*H*). $^{13}C\{_1H\}$ NMR (125 MHz, d_6-DMSO) δ: 12.2 ($NCH_2CH(CH_3)_2$), 20.7 ($NCH_2CH(CH_3)_2$), 51.1 ($NCH_2CH(CH_3)_2$), 52.3 (benzylic CH_2), 117.3, 122.3, 124.9, 133.8 (Ar-*C* benzyl), 116.1, 120.8, 123.6, 134.3, 135.3, (Ar-*C* benzimidazole), 179.7 (benzimidazolium *C2′*-Ag). FT-IR (KBr disc) cm^{-1}: ~2925, 2838 ν(C–H), 1594 ν(C=N, benzimidazole), 1012 ν(C–N, benzimidazole). *Anal.* Calc. for $C_{36}H_{40}N_4AgBr$: C, 60.3; H, 5.6; N, 7.8. Found: C, 60.5; H, 6.0; 7.9%.

2.2.7. Synthesis of bis-[1-benzyl-3-(2′-methyl)butylbenzimidazolium] silver(I) bromide (**7**)

This complex was prepared in a manner analogous to that for complex **6**, only with the benzimidazolium salt **2** (0.359 g, 1.0 mmol) instead of salt **1**. Further work up and purification of this complex were done in a methanol/*n*-hexane mixture. Yield: 48.4%. M.P.: >300 °C. ^1H NMR (500 MHz, d_6-DMSO) δ: 1.01 (12H, d J = 6.5 Hz, 2 × $NCH_2CH_2CH(CH_3)_2$), 2.01–2.10 (2H, m, 2 × $NCH_2CH_2CH(CH_3)_2$), 3.41 (4H, quart J = 5.5 Hz, 2 × $NCH_2CH_2CH(CH_3)_2$), 4.79 (4H, t J = 6.2 Hz,2 × $NCH_2CH_2CH(CH_3)_2$), 5.96 (4H, s, 2 × benzylic CH_2), 7.24–7.32 (10H, m, benzyl-*H*), 7.72–7.81 (2H, m, benzimidazole-*H*), 8.11–8.19 (2H, m, benzimidazole-*H*). $^{13}C\{^1H\}$ NMR (125 MHz, d_6-DMSO) δ: 11.0 ($NCH_2CH_2CH(CH_3)_2$), 22.2 ($NCH_2CH_2CH(CH_3)_2$), 30.1 ($NCH_2CH_2CH(CH_3)_2$), 51.5 ($NCH_2CH_2CH(CH_3)_2$), 52.7 (benzylic CH_2), 118.4, 119.8, 123.3, 133.0 (Ar-*C* benzyl), 116.6, 123.9, 125.1, 132.0, 134.2 (Ar-*C* benzimidazole), 181.5 (benzimidazolium *C2′*-Ag). FT-IR (KBr disc) cm^{-1}: 2933, ~2875 ν(C–H), 1582 ν(C=N, benzimidazole), ~1010 ν(C–N, benzimidazole). *Anal.* Calc. for $C_{38}H_{44}N_2AgBr$: C, 61.3; H, 6.0; N, 7.5. Found: C, 61.0; H, 6.3; 7.2%.

2.2.8. Synthesis of bis-[1-benzyl-3-hexylbenzimidazolium]silver(I) bromide (**8**)

This complex was prepared in a manner analogous to that for complex **6**, only with the benzimidazolium salt **3** (0.373 g, 1.0 mmol) instead of salt **1**. Further work up and purification of this complex were done in a methanol/*n*-hexane mixture. Yield: 57.7%. M.P.: >300 °C. ^1H NMR (500 MHz, d_6-DMSO) δ: 0.92 (6H, t J = 6.8 Hz, 2 × $N(CH_2)_5CH_3$), 1.26–1.35 (4H, m, 2 × $N(CH_2)_4CH_2CH_3$), 2.17–2.24 (4H, quart, 2 × $N(CH_2)_3CH_2CH_2CH_3$),

2.89–2.96 (4H, quart, 2 × $N(CH_2)_2CH_2(CH_2)_2CH_3$), 3.65–3.71 (4H, quart, 2 × $NCH_2CH_2(CH_2)_3CH_3$), 4.83 (4H, t J = 6.0 Hz, 2 × $NCH_2(CH_2)_4CH_3$), 5.89 (4H, s, 2 × benzylic CH_2), 7.33–7.40 (6H, m, benzyl-*H*), 7.52–7.60 (4H, m, benzyl-*H*), 7.95 (4H, t J = 7.0 Hz, benzimidazole-*H*), 8.20–8.28 (4H, m, benzimidazole-*H*). $^{13}C\{^1H\}$ NMR (125 MHz, d_6-DMSO) δ: 10.8 ($N(CH_2)_5CH_3$), 18.0 ($N(CH_2)_4CH_2CH_3$), 22.2 ($N(CH_2)_3CH_2CH_2CH_3$), 29.3 ($N(CH_2)_2CH_2(CH_2)_2CH_3$), 36.1 ($NCH_2CH_2(CH_2)_3CH_3$), 51.8 ($NCH_2(CH_2)_4CH_3$), 52.9 (benzylic CH_2), 116.1, 118.4, 123.6, 134.1 (Ar-*C* benzyl), 117.1, 124.5, 133.0, 135.1 (Ar-*C* benzimidazole), 188.3 (benzimidazolium *C*2′-Ag). FT-IR (KBr disc) cm^{-1}: 2928, ~2855 ν(C–H), 1598 ν(C=N, benzimidazole), 1017 ν(C–N, benzimidazole). *Anal.* Calc. for $C_{40}H_{48}N_4AgBr$: C, 62.2; H, 6.3; N, 7.2. Found: C, 62.7; H, 6.5; 7.5%.

2.2.9. Synthesis of bis-[1-benzyl-3-(2′-methyl)propylbenzimidazolium] palladium(II)chloride (**9**)

To a solution of bis-NHC silver(I) bromide complex **6** (0.358 g, 0.05 mmol) in dichloromethane (25 mL) was added [$PdCl_2(CH_3CN)_2$] (0.130 g, 0.05 mmol). The mixture was stirred for 12 h at room temperature in the dark. The resultant suspension was filtered through a bed of Celite and the volume of the filtrate was reduced on a rotary evaporator to 5 mL. Further addition of diethyl ether to the filtrate afforded the bis-NHC palladium(II) complex **9** as a pale brown powder which was filtered, washed with fresh diethyl ether (2 × 3 mL) and recrystallized from methanol/diethyl ether. Yield: 76.4%. M.P.: >300 °C. ^1H NMR (500 MHz, d_6-DMSO) δ: 0.82 (12H, d J = 7.0 Hz, 2 × $NCH_2CH(CH_3)_2$), 1.81–1.89 (2H, m, 2 × $NCH_2CH(CH_3)_2$), 4.30 (4H, t J = 7.0 Hz, 2 × $NCH_2CH(CH_3)_2$), 5.77 (4H, s, benzylic CH_2), 7.38–7.46 (10H, m, benzyl-*H*), 7.61–7.68 (4H, m, benzimidazole-*H*), 7.82–7.90 (4H, m, benzimidazole-*H*). $^{13}C\{^1H\}$ NMR (125 MHz, d_6-DMSO) δ: 11.0 ($NCH_2CH(CH_3)_2$), 18.1 ($NCH_2CH(CH_3)_2$), 50.8 ($NCH_2CH(CH_3)_2$), 52.0 (benzylic CH_2), 116.0, 118.6, 122.7, 134.0 (Ar-*C* benzyl), 117.5, 123.8, 124.4, 135.0, 135.7, (Ar-*C* benzimidazole), 172.0 (benzimidazolium *C*2′-Pd). FT-IR (KBr disc) cm^{-1}: ~2950, 2822 ν(C–H), 1581 ν(C=N, benzimidazole), 1048 ν(C–N, benzimidazole). *Anal.* Calc. for $C_{36}H_{40}N_4PdCl_2$: C, 61.2; H, 5.7; N, 7.9. Found: C, 61.5; H, 6.1; 8.0%.

2.2.10. Synthesis of bis-[1-benzyl-3-(2′-methyl)butylbenzimidazolium] palladium(II)chloride (**10**)

This complex was prepared in a manner analogous to that for complex **9**, only with the bis-NHC silver(I) complex **7** (0.37 g, 0.05 mmol) instead of complex **6**. Yield: 61.6%. M.P.: >300 °C. ^1H NMR (500 MHz, d_6-DMSO) δ: 0.88 (12H, d J = 6.2 Hz, 2 × $NCH_2CH_2CH(CH_3)_2$), 1.91–2.00 (2H, m, 2 × $NCH_2CH_2CH(CH_3)_2$), 3.21–3.26 (4H, quart J = 5.2 Hz, 2 × $NCH_2CH_2CH(CH_3)_2$), 4.69 (4H, t J = 6.2 Hz,2 × $NCH_2CH_2CH(CH_3)_2$), 5.91 (4H, s, 2 × benzylic CH_2), 7.18–7.27(10H, m, benzyl-*H*), 7.60–7.68 (2H, m, benzimidazole-*H*), 7.95–8.03 (2H, m, benzimidazole-*H*). $^{13}C\{^1H\}$ NMR (125 MHz, d_6-DMSO) δ: 13.1 ($NCH_2CH_2CH(CH_3)_2$), 19.8 ($NCH_2CH_2CH(CH_3)_2$), 33.7 ($NCH_2CH_2CH(CH_3)_2$), 51.0 ($NCH_2CH_2CH(CH_3)_2$), 52.76 (benzylicCH_2), 116.9, 118.0, 122.3, 134.1 (Ar-*C* benzyl), 117.5, 123.6, 124.7, 134.0, 135.1, (Ar-*C* benzimidazole), 175.7 (benzimidazolium *C*2′-Pd). FT-IR (KBr disc) cm^{-1}: 2948, ~2850 ν(C–H), 1597 ν(C=N, benzimidazole), 1027 ν(C–N, benzimidazole). *Anal.* Calc. for $C_{38}H_{44}N_2PdCl_2$: C, 62.2; H, 6.0; N, 7.6. Found: C, 62.6; H, 6.5; 7.9%.

2.2.11. Synthesis of bis-[1-benzyl-3-hexylbenzimidazolium] palladium(II) chloride (**11**)

This complex was prepared in a manner analogous to that for complex **9**, only with the bis-NHC silver(I) complex **8** (0.372 g, 0.05 mmol) instead of complex **6**. Yield: 68.7%. M.P.: >300 °C.^1H NMR (500 MHz, d_6-DMSO) δ: 1.01 (6H, t J = 7.0 Hz, 2 × $N(CH_2)_5CH_3$), 1.20–1.28 (4H, m, 2 × $N(CH_2)_4CH_2CH_3$), 2.06–2.14 (4H, quart, 2 × $N(CH_2)_3CH_2CH_2CH_3$), 2.66–2.71 (4H, quart, 2 × $N(CH_2)_2CH_2(CH_2)_2CH_3$), 3.80–3.87 (4H, quart, 2 × $NCH_2CH_2(CH_2)_3CH_3$), 4.98 (4H, t J = 6.2 Hz, 2 × $NCH_2(CH_2)_4CH_3$), 6.03 (4H, s, 2 × benzylic CH_2), 7.20–7.28 (6H, m, benzyl-*H*), 7.61–7.68 (4H, m, benzyl-*H*), 7.90 (4H, t J = 6.0 Hz, benzimidazole-*H*), 8.23–8.29 (4H, m, benzimidazole-*H*). $^{13}C\{^1H\}$ NMR (125 MHz, d_6-DMSO) δ: 13.1 ($N(CH_2)_5CH_3$), 19.4 ($N(CH_2)_4CH_2CH_3$), 24.2 ($N(CH_2)_3CH_2CH_2CH_3$), 27.9 ($N(CH_2)_2CH_2(CH_2)_2CH_3$), 38.0 ($NCH_2CH_2(CH_2)_3CH_3$), 50.3 ($NCH_2(CH_2)_4CH_3$), 51.8 (benzylic CH_2), 117.3, 118.8, 124.3, 133.3 (Ar-*C* benzyl), 122.2, 123.1, 134.2, 135.6 (Ar-*C* benzimidazole), 173.2 (benzimidazolium *C*2′-Pd). FT-IR (KBr disc) cm^{-1}: 2933, ~2880 ν(C–H), 1591 ν(C=N, benzimidazole), 1008 ν(C–N, benzimidazole). *Anal.* Calc. for $C_{40}H_{48}N_4PdCl_2$: C, 63.0; H, 6.4; N, 7.4. Found: C, 63.1; H, 6.7; 7.0%.

2.3. DFT calculations

GAUSSIAN 09 [15] was used to perform all the theoretical calculations. The structures of the isomers were built based on the crystal structure of the similar complex (trans-bis[1-benzyl-3-(2,3,4,5,6-pentafluorobenzyl)benzimidazol-2-ylidene]dibromopalladium(II)), a palladium complex with a substituted benzimidazole ligand [16]. The 6-31G(d,p) basis set was used for the atoms C, H, N and Cl, while Pd was described with LANL2DZ basis set. The optimisation was carried out without any restriction in symmetry or internal coordinates. Frequencies calculations have shown no imaginary frequencies, hence the optimized structures are in their optimum minima. The optimized structures were used to calculate the full set of molecular orbitals, however we are going to focus on the orbitals from HOMO−2 to LUMO+2 and the band gap energy (LUMO−HOMO).

2.4. Catalytic olefin oxidation studies

The epoxidation of the olefins 1-octene and styrene with 30% aqueous hydrogen peroxide was performed in a 25 mL round bottom flask equipped with a condenser. In a typical epoxidation experiment, the flask was charged with 10 mL of acetone (or acetonitrile/dichloromethane), 1.0 mmol olefin as the substrate, 1.0 mmol hydrogen peroxide as the oxidant and 1.0 mmol of complex **9**–**11** as the catalyst. The reaction was carried out in an oil bath under stirring at a constant temperature of 70 °C for 4 h. After every hour, aliquots were removed and analyzed immediately with a GC instrument. Before analysis, these aliquots were treated with diethyl ether and centrifuged to remove unreacted hydrogen peroxide, water and catalyst. The organic part was subsequently separated and analyzed by the GC instrument. Olefin conversion (%) and the reaction products were quantified by GC and identified by comparison with the retention time to those of authentic standard samples.

3. Results and discussion

In the present work a series of new palladium(II)–NHC-complexes of 1,3-dialkyl-aryl substituted benzimidazol-2-lyidenes is presented. All the synthesized compounds were stable towards air and moisture, while the silver complexes were found to be light sensitive. All the compounds are insoluble in water (except **4** and **5**), but readily soluble in common organic solvents, like DMF, DMSO, methanol, acetone, dichloromethane and acetonitrile. The bis-NHC palladium(II) complexes were used as homogeneous catalysts for olefin epoxidation reactions as the focus of the present work. A quantitative correlation is drawn between the changes in the steric bulk around the metal center and their activity towards olefin oxidations. Microanalysis data of all the synthesized compounds agree well with their proposed structures. Although it was demonstrated that the palladium(0/II)–NHC complexes could

easily be obtained via transmetallation from their silver(I) counterparts and isolated in almost quantitative yields, it seems that these complexes have been largely ignored until recently for application as olefin oxidation catalysts.

3.1. Syntheses

The reaction of 1*H*-benzimidazole and benzyl bromide in the presence of a strong base resulted in the formation of 1-benzylbenzimidazole [14], which was exploited for connecting N-alkyl groups such as 2-methylpropyl, 2-methylbutyl and hexyl to afford a series of 1-benzyl-3-alkylbenzimidazolium bromide salts, **1**–**3**, in good yield. Analogously, using standard Schlenk techniques, 1-butylimidazole and 1-butylbenzimidazole were prepared and treated with an equimolar amount of cyanuric chloride at ice temperature in dry acetone under nitrogen atmosphere to afford 2,4,6-triazine-functionalized 1-butylimidazolium and benzimidazolium salts **4** and **5**, respectively, in good yield as shown in Scheme 1. This new ligand set was fully characterized using different spectral and analytical tools, and the molecular structure of the imidazolium salt **4** was confirmed by the single-crystal X-ray diffraction technique.

With a mono carbene carbon coordination site potentially available for hosting a palladium ion, the benzimidazolium salts **1**–**5** were reacted with $[PdCl_2(CH_3CN)_2]$ at different stoichiometric ratios, reaction conditions and solvents over different reaction periods, but this did not result in any complex formation. Therefore, we followed the carbene transfer method [17] to prepare the desired sterically modulated palladium(II)–NHC complexes. With use of the *in situ* deprotonation method [18], the benzimidazolium salts **1**–**3** were treated with half an equivalent of silver oxide in stirring methanol at room temperature for 48 h in the dark, yielding the colorless silver(I)–NHC complexes, **6**–**8**, respectively. All of these silver derivatives were fully characterized by elemental analysis, FT-IR and ^1H and ^{13}C NMR spectroscopy. These complexes were formed in good yield. The reactions involved in the preparation of the silver(I) complexes **6**–**8** are shown in Scheme 2. Conversely, the reactions of imidazolium and benzimidazolium salts **4** and **5** under the same and many other

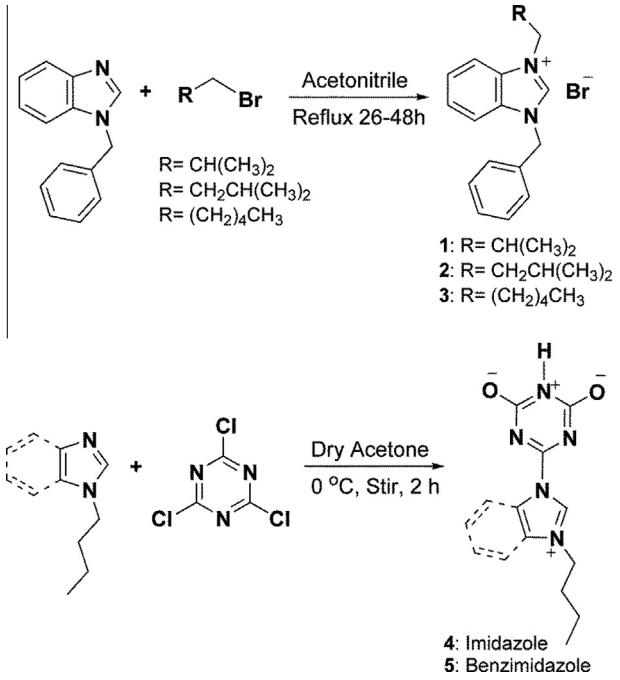

Scheme 1. Synthesis of the sterically modulated (benz)imidazol-2-ylidenes.

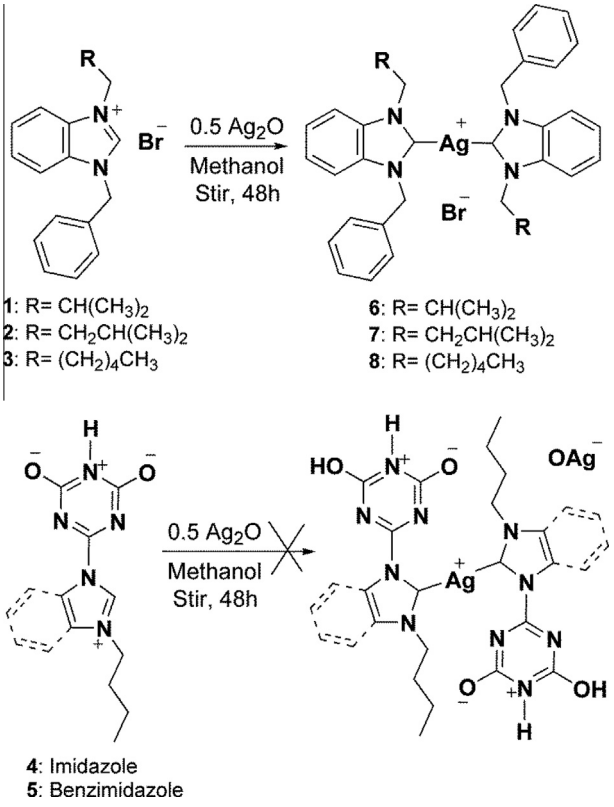

Scheme 2. Synthesis of the sterically modulated silver(I)–NHC complexes.

reaction conditions resulted in no silver(I) complex formation due to the low acidity of the C2 proton. This inactivity of compounds **4** and **5** towards complex formation could be attributed to the insertion of the triazine moiety, which perhaps made the C2 proton less acidic, that in turn did not allow the deprotonation of the C2 proton.

The synthesis of palladium(II)–NHC complexes **9**–**11** was accomplished *via* the transmetallation method [19] by treating equimolar amounts of the silver(I)–NHC complexes **6**–**8** with $[PdCl_2(CH_3CN)_2]$ in dichloromethane at room temperature, overnight under the exclusion of light. The desired complexes **9**–**11** were purified by repeated precipitation in methanol/diethyl ether. The palladium complexation reactions proceeded smoothly to afford neutral palladium(II) complexes **9**–**11** in around 61–76% isolated yields. These title complexes were obtained as pale green to brown powders and were fully characterized by elemental analysis, FT-IR and ^1H and ^{13}C NMR spectral techniques. The reactions involved in the formation of these complexes are outlined in Scheme 3.

3.2. Spectral characterization

Successful formation of the NHC precursor salts **1**–**5** and their carbene complexes **6**–**11** in each step can be nicely traced by spectroscopic methods, followed by microanalysis data. In the FTIR spectra of the silver(I) and palladium(II) complexes **6**–**11**, the $\nu_{C=N}$ stretching frequencies upon coordination shifted to lower values (1582–1598 cm^{-1}) in comparison to those of the benzimidazolium salts (1612–1628 cm^{-1}) [20]. Notably, the corresponding ν_{C-N} stretching frequencies followed the same trend. Upon coordination to the metal center, the ν_{C-N} vibrations shifted to lower values (1008–1048 cm^{-1}) in comparison to those of the benzimidazolium salts (1050–1101 cm^{-1}). These observations are collectively attributed to the successful complex formation. In the case of the

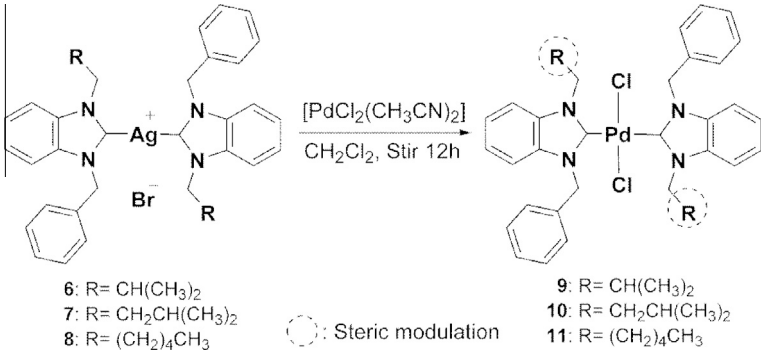

Scheme 3. Synthesis of the sterically modulated Pd–NHC complexes *via* the transmetallation technique.

triazine-tethered (benz)imidazolium salts, **4** and **5**, an additional medium intensity band at 1628 and 1621 cm^{-1} was observed respectively, due to the $\nu_{C=N}$ stretching frequencies originating from the triazine core. The spectra also evidenced the presence of two medium intensity sharp bands at around 2860 and 2930 cm^{-1}, attributed to the stretching vibrations of both aliphatic and aromatic C–H bonds.

The NMR spectroscopic characterization of both the NHC precursors and their carbene complexes was assisted by a combination of ^{1}H and ^{13}C NMR spectroscopic experiments. Data from room temperature ^{1}H and ^{13}C NMR spectroscopic investigation for compounds **1–11** was collected using d_6-dimethylsulfoxide/D_2O solution. The successful formation of benzimidazolium salts **1–3** was confirmed by the downfield benzimidazolium-C2-ptoton signal at δ10.12, 9.92 and 10.05 respectively, followed by relatively less low field aromatic proton resonances in the range δ 7.01–8.11. Signals for the protons bound to the 2-methylpropyl, 2-methylbutyl and n-hexyl chains appear in the range δ 0.88–4.8, which are in good agreement with the literature [21]. The ^{13}C NMR spectra of salts **1–3** exhibit characteristic downfield resonances at δ 140.2, 139.4 and 137.7 respectively for the benzimidazolium-C2 carbon nuclei. The spectra also show a set of upfield resonance signals in the range δ 11–52 and 116–134, assignable to the aliphatic and aromatic carbon nuclei, respectively. The successful formation of the silver(I) and palladium(II)–NHC complexes was confirmed by the absence of the resonance for the most downfield acidic benzimidazolium-C2 proton signals in the ^{1}H NMR spectra of the complexes. Further, the ^{13}C NMR spectra of the carbene complexes **6–11** reveal a significant downfield shift of the benzimidazolium-C2 signal at δ 179.7, 181.5, 188.3, 172.0, 175.7 and 173.2, respectively, confirming coordination of the carbene carbon atom to the metal center. These observations are in good agreement with the data reported for carbene complexes having similar ligand architectures [22].

Siebert and co-workers reported [23] a series of imidazole-2-yldine based macrocycles and their inability to undergo carbene complexation when treated with $NiCl_2$, $Ni(OAc)_2$, $Pd(OAc)_2$ and $[(Ph_3P)_2PtCl_2]$. Further, they demonstrated the cause for the inactivity of the macrocycles towards complex formation is the low acidity of the imidazole C2 protons (δ 6.64–7.5 in CD_2Cl_2). In comparison with Siebert's work, we concluded that the inability of our Zwitterionic triazine-tethered (benz)imidazolium salts **4** and **5** to form silver(I)–NHC complexes was based, in part, on the low acidity of their C2 proton, whose resonance was found at δ 8.91 and 9.01 in D_2O, respectively. These chemical shift values of the C2 protons are in the upfield region compared to the C2 proton resonance of salts **1–3** by *ca* δ 1.

3.3. X-ray structural description of salt 4

The solid state structure of the Zwitterionic imidazolium salt **4** has been identified by the single crystal X-ray diffraction technique. Slow diffusion of diethyl ether into a methanolic solution of salt **4** yielded crystals suitable for single crystal X-ray diffraction analysis. The crystal data, structure refinement details, selected bond distances and angles of salt **4** are tabulated in Tables 1–3, respectively. The molecular structure of salt **4** in the solid state is depicted in Figs. 1 and 2.

The imidazolium salt **4** crystallizes in the monoclinic space group $P2_1/C$, with two crystallographically independent units (A and B) in the dibasic Zwitterionic form. Two crystallographically inequivalent dibasic salts and two water molecules occupy the asymmetric unit of salt **4** with a set of disordered butyl carbon atoms. In the formation of salt **4**, both the chloride atoms at the 3- and 5-positions of the triazine ring have undergone hydrolysis to form hydroxyl units, which in turn form the dibasic salt by ionization to balance the positive charges originating from quarternization at the imidazolium group and N2 of the triazine. It is interesting that both the triazine and imidazolium rings show π–π stacking interactions perpendicular to the *ab*-plane with triazine and imidazole rings of other molecules, with interaction bond distances of 3.372 and 3.372 Å, respectively. The triazine rings are slightly tilted from the associated imidazolium rings by a dihedral angle of 5.19(18)° and 15.04(18)° for the A and B units, respectively. The internal ring angles, N5A–C4A–N4A and N5B–C4B–N4B, at the carbene centers are found to be 107.64(14)° and 108.48(14)°,

Table 1
Crystal data and structure refinement details of the Zwitterionic imidazole salt **4**.

	4
Formula	$C_{20}H_{30}N_{10}O_6$
Formula weight	506.54
Crystal system	monoclinic
Space group	*P*2(1)/*c*
Unit cell dimensions	
a (Å)	13.7996(19)
b (Å)	9.9497(15)
c (Å)	20.955(2)
α (°)	90.00
β (°)	125.785(6)
γ (°)	90.00
V (Å^3)	2334.0(5)
Z	4
D_{calc} (g/cm^3)	1.442
Absorption coefficient (mm^{-1})	0.110
F(000)	1072
Crystal size (mm)	0.68 × 0.17 × 0.14
T (K)	100
Radiation (Å)	Mo Ka 0.71073
θ Min, max (°)	1.82, 30.07
Dataset	−19:19; −14:13; −29:29
Total Unique data	18868
R_{int}	0.0406
Nref, Npar	6782, 392
R, wR_2, S	0.0501, 0.1235, 1.043

Table 2
Selected bond distances (Å) of the crystallographically independent units, A and B, of the Zwitterionic salt **4**.

Unit A of ***4***			
C7A–N5A	1.464(2)	C3A–N1A	1.321(2)
N5A–C4A	1.329(2)	C1A–N1A	1.366(2)
N5A–C6A	1.383(2)	N3A–C2A	1.365(2)
C4A–N4A	1.3491(18)	C2A–N2A	1.376(2)
C5A–N4A	1.390(2)	C1A–N2A	1.3887(18)
C3A–N4A	1.427(2)	C1A–O1A	1.237(2)
C3A–N3A	1.3209(18)	C2A–O2A	1.2409(17)
Unit B of ***4***			
C7B–N5B	1.472(2)	C3B–N1B	1.316(2)
N5B–C4B	1.316(2)	C1B–N1B	1.365(2)
N5B–C6B	1.3920(19)	N3B–C2B	1.369(2)
C4B–N4B	1.3444(18)	C2B–N2B	1.373(2)
C5B–N4B	1.382(2)	C1B–N2B	1.3852(19)
C3B–N4B	1.433(2)	C1B–O1B	1.241(2)
C3B–N3B	1.3200(17)	C2B–O2B	1.2454(18)

Table 3
Selected bond angles (°) of the crystallographically independent units, A and B, of the Zwitterionic salt **4**.

Unit A of ***4***			
C7A–N5A–C4A	124.71(14)	C3A–N3A–C2A	114.09(14)
C7A–N5A–C6A	125.49(16)	N3A–C2A–O2A	121.76(15)
C6A–N5A–C4A	109.28(14)	N1A–C1A–O1A	122.86(14)
N5A–C4A–N4A	107.64(14)	O1A–C1A–N2A	120.09(17)
C4A–N4A–C3A	124.07(14)	O2A–C2A–N2A	120.19(17)
N4A–C3A–N3A	113.69(14)	C2A–N2A–C1A	123.76(16)
N4A–C3A–N1A	114.17(13)	N2A–C1A–N1A	117.05(15)
C3A–N1A–C1A	114.74(13)	N2A–C2A–N3A	118.05(13)
Unit B of ***4***			
C7B–N5B–C4B	125.36(14)	C3B–N3B–C2B	113.32(14)
C7B–N5B–C6B	125.59(16)	N3B–C2B–O2B	122.24(16)
C6B–N5B–C4B	109.02(13)	N1B–C1B–O1B	123.18(14)
N5B–C4B–N4B	108.48(14)	O1B–C1B–N2B	119.73(17)
C4B–N4B–C3B	123.54(14)	O2B–C2B–N2B	119.32(17)
N4B–C3B–N3B	113.56(14)	C2B–N2B–C1B	123.57(16)
N4B–C3B–N1B	113.79(13)	N2B–C1B–N1B	117.07(15)
C3B–N1B–C1B	114.72(13)	N2B–C2B–N3B	118.44(13)

respectively, which are consistent with earlier reports [24]. In the extended crystal structure (Fig. 3), the dibasic units of **4** are connected *via* three types of hydrogen bonds, viz.,

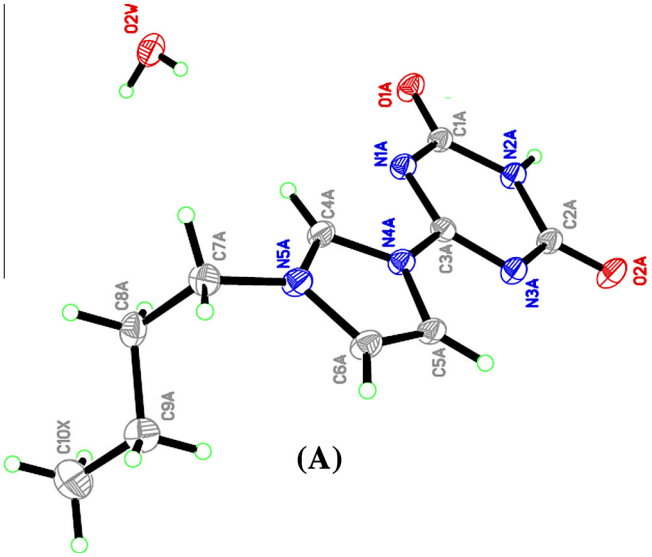

Fig. 1. Molecular structure of the triazine-functionalized imidazolium-2-ylidene **4** (unit A) showing 50% probability thermal ellipsoids.

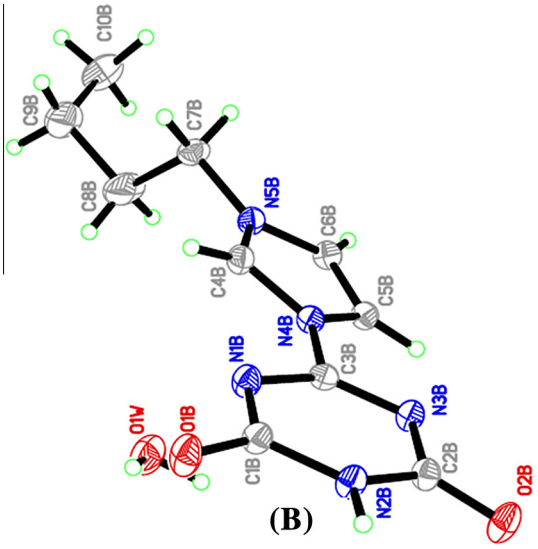

Fig. 2. Molecular structure of the triazine-functionalized imidazolium-2-ylidene **4** (unit B) showing 50% probability thermal ellipsoids.

HO---$O_{trizine}$ (1.998 Å), $CH_{imidazolium}$---$O_{triazine}$ (2.569 Å) and OH---O_{water} (2.103 Å), forming a three-dimensional network. Further, the molecules of **4** possess numerous short contacts between heteroatoms and the disordered and non-disordered hydrogen atoms, with bond distances ranging from 2.880 to 3.357 Å. These bond distances are quite normal and are comparable to the reported values of similar imidazolium salts [25].

3.4. Theoretical studies on complexes *9* and *11* using the DFT method

DFT studies have been performed to understand the structures of the targeted complexes. The theoretical parameters for complexes **9** and **11** in the gaseous phase, such as the nature of the molecular orbitals, HOMO and LUMO, and the cis–trans energy barrier, have been established by this study using the B3LYP method. Gökçe and co-workers reported the synthesis and crystal structure of a similar complex, trans-bis[1-benzyl-3-(2,3,4,5,6-pentafluorobenzyl)benzimidazol-2-ylidene] dibromopalladium(II) [16]. The palladium(II) centre in this complex is conjugated with two bromide atoms and two substituted benzimidazole groups. The benzyl group and the pentafluorobenzyl unit on each benzimidazole entity form a trans-conformation. Since the palladium complexes in this report similarly form complexes with 1,3-disubstituted benzimidazole groups and two chlorido ligands, it is appropriate to build the complexes **9** and **11** accordingly. B3LYP, as one of the density functional methods, was used to optimize the starting structures. The common bond distances, angles and dihedral angles were compared with the crystal structure from the literature, Table 4.

The electronic energies of the optimized complexes in both conformations, cis- and trans-, are listed in Table 5. Interestingly, the energy difference between the cis- and trans-conformations has shown that the trans-isomer is slightly preferable by 1.2 kcal/mol for complex **9** and 0.6 kcal/mol for complex **11**. It is obvious that the values of the energy differences between the two conformations for the two complexes are small, around 1 kcal/mol, and hence it is difficult to say that the cis-conformers of the two complexes are more stable than the trans-conformers. Experimentally, the separation difficulty of the two isomers of the complexes might be due to the low energy difference between them. A similar observation is reported in case of rhenium(I)–NHC complexes [26].

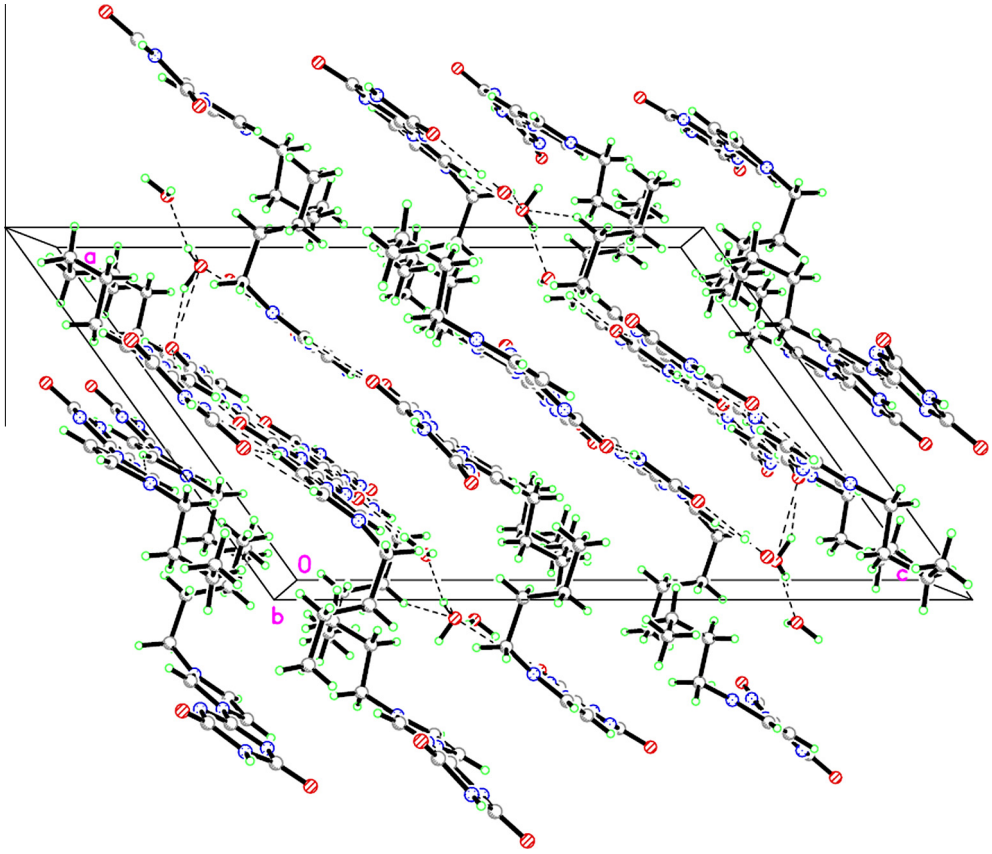

Fig. 3. Crystal packing diagram of the triazine-functionalized imidazolium-2-ylidene **4** showing C–H···O, C–H···N and O–H···O hydrogen bonds.

The optimized structures of the studied complexes were used to calculate the energies of the molecular orbitals (MOs). In order to have a general idea about the molecular orbitals, a number of orbitals beside the HOMO and LUMO orbitals are shown in Fig. 4. The energies of the molecular orbitals and the density distribution may give some insight into the reactivity and kinetic stability of the isomers. In addition, the energies of the HOMO and LUMO represent the molecule's ability to donate or accept an electron, respectively. Fig. 4 shows the molecular orbitals HOMO−2 to LUMO+2 and the band gaps for the cis- and trans-conformations of complexes **9** and **11**. The band gaps for the two complexes **9** and **11** are very close, 1.6 and 1.7 eV, respectively.

The molecular density distribution through the molecular orbitals reflects the contribution of each atom in a molecular orbital. The localization of the density for the HOMO and LUMO for each of the two complexes is summarized in Figs. 5 and 6. Interestingly, the density localization is identical for the corresponding molecular orbitals for the two complexes. The highest contribution for the HOMO molecular orbital for the two isomers is attributed to the lone pairs on the chlorido ligands. In the LUMO orbital, in addition to the localized density from palladium(II) and the two chlorido ligands, there is some contribution from the carbene carbon atom of the benzimidazole-2-ylidene groups, as shown in Figs. 5 and 6.

Table 4
Bond distances (Å) and angles (°) for the optimized structures of complexes **9** and **11**.

Bond distance/angle	**9**		**11**	
	cis-	trans-	cis-	trans-
Pd–Cl	2.39	2.395	2.387	2.392
Pd–$C_{carbene}$	2.066	2.07	2.06	2.063
C–N (benzimi)	1.358	1.362	1.359	1.359
N–CH_2 (arom)	1.465	1.463	1.464	1.464
N–CH_2 (aliph)	1.468	1.471	1.464	1.465
Cl–Pd–C	89.5	88.9	89.9	89.7
Pd–C–N	125.2	124.7	126.8	126.3
Cl–Pd–C–N	77.9	71.1	74.8	72.6

3.5. Catalytic epoxidation studies of complexes *9–11*

After obtaining an insight into the coordination behavior of the carbene ligands in the palladium(II)–NHC complexes **9–11** from the aforementioned spectral and analytical studies, we undertook an investigation to access their performances in the catalytic olefin epoxidation of 1-octene and styrene using aqueous hydrogen peroxide as an oxidant in homogeneous medium. The blank experiments without **9–11** show no formation of epoxide or any other oxidized products with either with 1-octene or with styrene. Therefore, it is believed that the catalytic performances displayed are mainly due to the presence of active species of **9–11**. The catalytic performances of **9–11** in the epoxidation of 1-octene and styrene are summarized in Tables 6 and 7, respectively. As is evident from the aforementioned tables, the results of **9–11** towards the olefins differed significantly due to the different activity of the

Table 5
Electronic and relative energies for complexes **9** and **11** according to DFT.

Complex	Energy (Hartree)	Relative energy (Hartree)	Relative energy (kcal/mol)
cis-**9**	−2661.554654	0.00000	–
trans-**9**	−2661.556486	0.00183	1.1908
cis-**11**	−2818.712916	0.00000	–
trans-**11**	−2818.713806	0.00089	0.5785

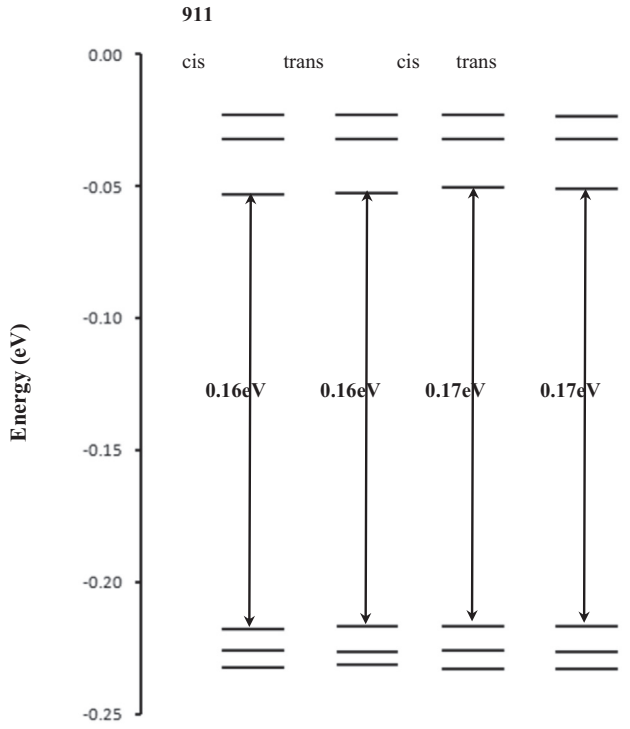

Fig. 4. Energy of the molecular orbitals for HOMO−2 through to LUMO+2 and band gaps for the cis and trans conformations of complexes **9** and **11**.

double bonds. Epoxidation of a linear aliphatic olefin, such as 1-octene, by **9**–**11** displayed 42–58% conversion and 9.5–17% 1,2-epoxyoctane selectivity because of its highly active double bond and the relative stability of the formed epoxide. However, in the case of epoxidation of an exocyclic olefin, such as styrene, only 13–19% conversion was observed with 100% selectivity towards epoxide formation, which was the sole product in this case. The catalytic reactions in the epoxidation of 1-octene by **9**–**11** are outlined in the Scheme 4.

In order to get more insight on the catalytic behavior of palladium(II) complexes, we have tuned the steric bulk (2-methylpropyl, 2-methylbutyl and n-hexyl) at one N-terminal of the benzimidazole core, keeping the other (benzyl) constant. Varied steric bulk around the active species of **9**–**11** affects the epoxidation activity in the order **9** (2-methylpropyl) > **10** (2-methylbutyl) > **11** (*n*-hexyl) towards both the olefins. Complex **9** provides comparatively less steric bulk around the active palladium centers allowing 1-octene and styrene conversion up to 58% and 19%, respectively, with a much higher selectivity profile. Conversely, in the case of complexes **10** and **11** the steric bulk around the active palladium species is much higher, and as a result the % conversion of 1-octene and styrene into their corresponding oxidized products was found to be 46.5%, 42% and 14.5%, 13% respectively, which is much less compared to complex **9**. This phenomenon also affected the selectivity of the epoxide formation of 1-octene, with 12 and 9.5% as the selectivity values [27]. This may due to the large hexyl/2-methylbutyl group of **10/11** connected to the benzimidazole N-terminal which sterically hinders the olefin approach towards the active site, while complex **9** with a smaller propyl group can provide access to the olefin with some ease for the formation of the epoxide. In all the cases of 1-octene epoxidation, the epoxide was the minor product, whereas, 1,2-octanediol and 2-octanone were the major constituents. Similar observations were observed in the literature for numerous heterogeneous catalysts [28]. The percentage conversion of 1-octene and the formation of

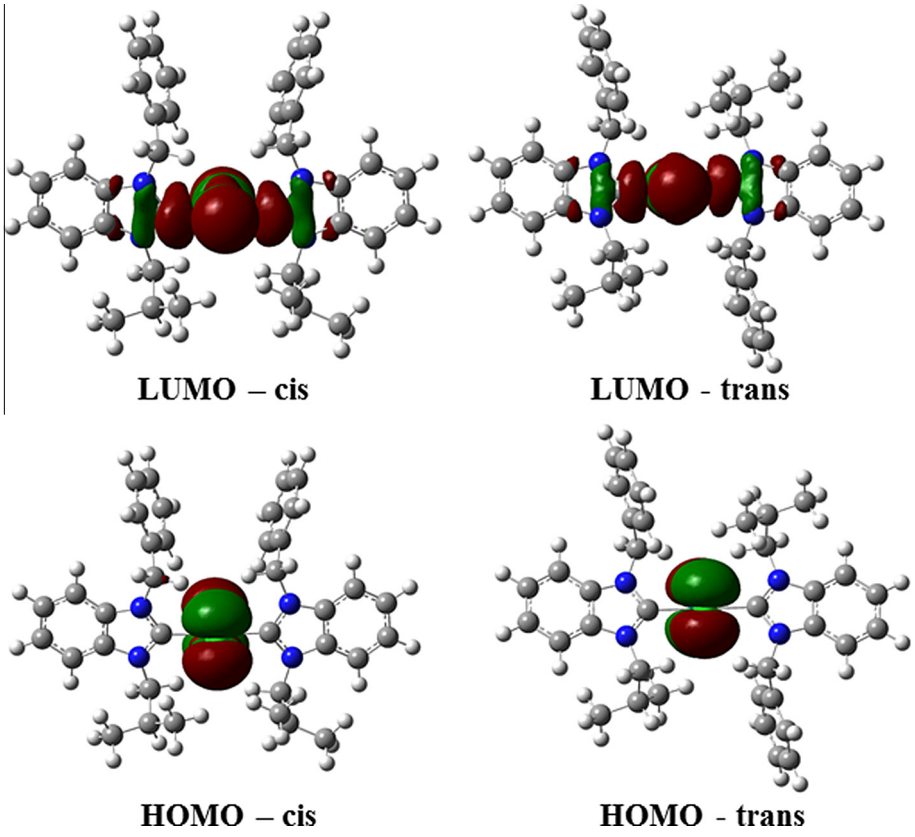

Fig. 5. Density distribution for the HOMO and LUMO for complex **9**.

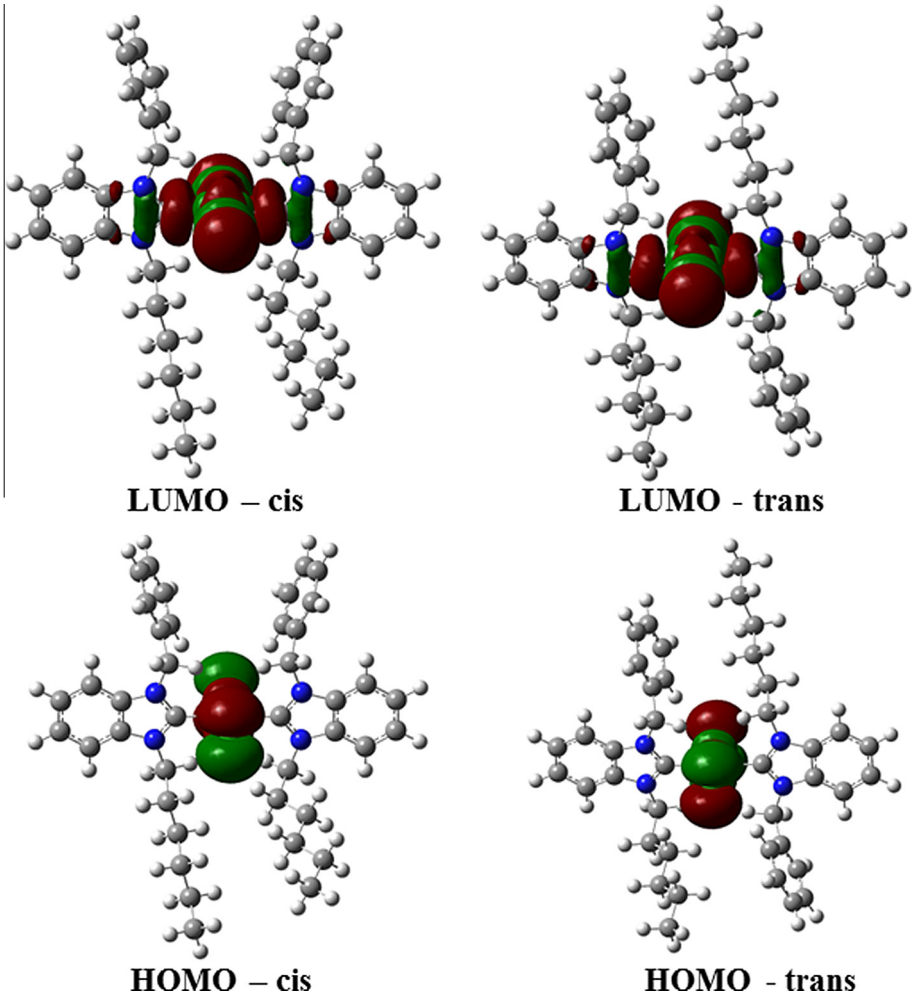

Fig. 6. Density distribution for the HOMO and LUMO for complex **11**.

Table 6
Catalytic performance of the palladium complexes **9**–**11** in 1-octene epoxidation.

Entry	Catalyst	Time (h)	Oxidant	% Conversion	% Selectivity		
					1,2-Octanediol	2-Octanone	1,2-Epoxyoctane
1	**1**	4	H_2O_2	–	–	–	–
2	**2**	4	H_2O_2	–	–	–	–
3	**3**	4	H_2O_2	–	–	–	–
4	**9**	4	–	–	–	–	–
5	**10**	4	–	–	–	–	–
6	**11**	4	–	–	–	–	–
7	**9**	1	H_2O_2	4.0	51.0	49.0	–
8	**9**	2	H_2O_2	14.5	58.0	42.0	trace[a]
9	**9**	3	H_2O_2	32.5	60.5	36.0	3.5
10	**9**	4	H_2O_2	58.0	61.0	22.0	17.0
11	**10**	1	H_2O_2	7.5	43.0	57.0	–
12	**10**	2	H_2O_2	10.0	44.5	55.5	trace[a]
13	**10**	3	H_2O_2	38.5	46.5	49.0	4.5
14	**10**	4	H_2O_2	46.5	43.0	45.0	12.0
15	**11**	1	H_2O_2	6.5	63.5	36.5	–
16	**11**	2	H_2O_2	16.5	67.0	33.0	–
17	**11**	3	H_2O_2	40.0	68.5	28.5	3.0
18	**11**	4	H_2O_2	42.0	69.5	21.0	9.5

[a] Not determined.

1,2-octanediol and 2-octanone on oxidation using aqueous hydrogen peroxide at 70 °C catalyzed by palladium complexes **9**–**11** is shown in Fig. 7.

The aforementioned catalytic experiments were also performed at the lower temperature of 40 °C to study the effect of temperature on the catalytic efficacies of complexes **9**–**11**, however, no or

Table 7
Catalytic performance of the palladium complexes **9**–**11** in styrene epoxidation.

Entry	Catalyst	Time (h)	Oxidant	% Conversion	% Epoxide
1	**1**	4	H_2O_2	–	–
2	**2**	4	H_2O_2	–	–
3	**3**	4	H_2O_2	–	–
4	**9**	4	–	–	–
5	**10**	4	–	–	–
6	**11**	4	–	–	–
7	**9**	1	H_2O_2	–	–
8	**9**	2	H_2O_2	3.5	3.5
9	**9**	3	H_2O_2	12.5	12.5
10	**9**	4	H_2O_2	19.0	19.0
11	**10**	1	H_2O_2	–	–
12	**10**	2	H_2O_2	–	–
13	**10**	3	H_2O_2	7.5	7.5
14	**10**	4	H_2O_2	14.5	14.5
15	**11**	1	H_2O_2	–	–
16	**11**	2	H_2O_2	–	–
17	**11**	3	H_2O_2	8.5	8.5
18	**11**	4	H_2O_2	13.0	13.0

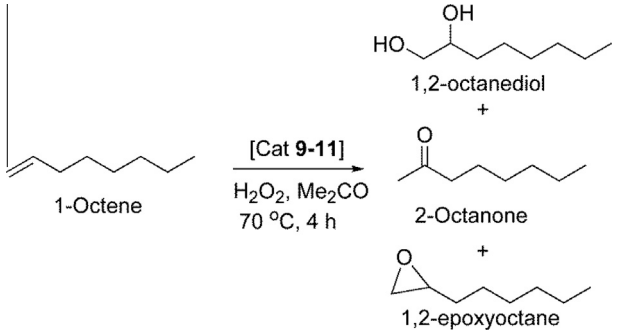

Scheme 4. Catalytic oxidation of 1-octene by the sterically modulated Pd(II)–NHC complexes **9**–**11** with hydrogen peroxide.

negligible product formations were found. On the other hand, the catalytic reactions were performed in a variety of solvents to study the catalytic efficacies of complexes **9**–**11** in different solvent media. The trend for the activity remains the same in all the solvents, whereas the efficiency of **9**–**11** decreased by 2.5–6% (1-octene) and 4.5–14.5% (styrene) in the order acetonitrile > acetone > dichloromethane. As is evident from Table 8, the activity in acetonitrile solvent was the best in all cases for both olefins. Both the variations in the reaction conditions, temperature and solvent, followed the general trend that the reaction rate was enhanced with an increase in the reaction temperature and polarity of the solvent. Similar results for various catalysts were found in the literature [29].

Table 8
Influence of solvent on the palladium complexes **9**–**11** catalyzed epoxidation reactions of olefins[b].

Entry	Catalyst	Substrate	% Conversion (% of epoxide formation)[c]		
			CH_3CN	CH_3COCH_3	CH_3Cl_2
1	**9**	1-octene	58.0 (17.0)	56.5 (17.0)	53.0 (14.5)
2	**9**	styrene	19	12.5	5.5
3	**10**	1-octene	46.5 (12.0)	44.0 (11.5)	40.5 (5.5)
4	**10**	styrene	14.5	11.0	5.0
5	**11**	1-octene	42.0 (9.5)	40.5 (9.0)	34.0 (3.5)
6	**11**	styrene	13	11.5	4.5

[b] % Yields of the products were calculated after 4 h of the reaction.
[c] In the case of styrene epoxidation, epoxystyrene is the sole product.

4. Conclusions

In summary, a series of sterically tuned palladium(II)–NHC complexes, **9**–**11**, were prepared by the technique of transmetallation from their silver(I) counterparts, **6**–**8**. The latter complexes were readily prepared by the reaction of silver(I) oxide with benzimidazolium salts, **1**–**3**, under mild conditions. The novel triazine-tethered (benz)imidazole salts **4** and **5** were prepared by the reaction of cyanuric chloride and *n*-butyl (benz)imidazole under inert conditions. The solid-state structure of the triazine-tethered Zwitterionic imidazolium salt **4** was determined by the single crystal X-ray diffraction method. However, metallation reactions of both the salts with silver oxide/palladium chloride under different reaction conditions ended with negative results due to the low acidity values of the azolium-C2 protons. Complexes **9**–**11** showed good catalytic activities for the olefin epoxidation reactions under homogeneous conditions with aqueous hydrogen peroxide as an oxidant. A change in the solvent affected the product formation, as reflected in the decreased % conversion of substrates in the order acetonitrile > acetone > dichloromethane. According to DFT calculations, the trans-isomers of complexes **9** and **11** are more favorable by 1.2 and 0.6 kcal/mol respectively.

Acknowledgments

N. Abdullah thanks the Malaysian Ministry of Higher Education for the Fundamental Research Grant Scheme (FP008-2011A). S. Endud thanks the Universiti Teknologi Malaysia (UTM) for the Research University grant Q.J130000.2513.05H20 and MOSTI for the National Nanotechnology Directorate Top-Down Grant R.J130000.7926.4H007. The authors thank the Ibnu Sina Institute for Fundamental Science Studies, UTM for research facilities.

Appendix A. Supplementary data

CCDC 901539 contains the supplementary crystallographic data for Zwitterionictriazinetethered imidazolium salt **4**. These data can

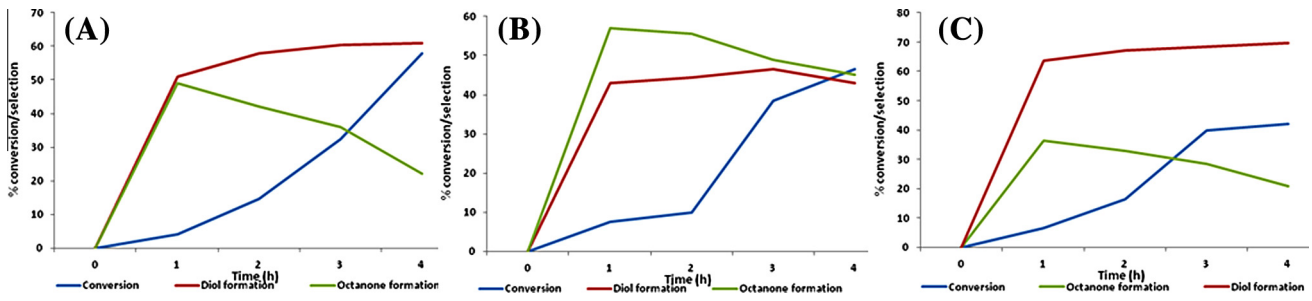

Fig. 7. Percentage conversion of 1-octene and the formation of 1,2-octanediol and 2-octanone from epoxidation using aqueous hydrogen peroxide at 70 °C catalyzed by palladium complexes **9** (A), **10** (B) and **11** (C).

be obtained free of charge via http://www.ccdc.cam.ac.uk/conts/retrieving.html, or from the Cambridge Crystallographic Data Centre, 12 Union Road, Cambridge CB2 1EZ, UK; fax: +44 1223 336 033; or e-mail: deposit@ccdc.cam.ac.uk.

References

[1] (a) S. Budagumpi, R.A. Haque, A.W. Salman, Coord. Chem. Rev. 256 (2012) 1787;
(b) S. Budagumpi, S. Endud, Organometallics 32 (2013) 1537;
(c) S.J. Hock, L.A. Schaper, W.A. Herrmann, F.E. Kuhn, Chem. Soc. Rev. 2013 (2013), http://dx.doi.org/10.1039/c3cs60019j;
(d) R.H. Crabtree, Coord. Chem. Rev. 257 (2013) 755;
(e) A. Kumar, P. Ghosh, Eur. J. Inorg. Chem. (2012) 3955;
(f) P.L. Arnold, S.T. Liddle, Chem. Commun. (2006) 3959.

[2] (a) W. Liu, R. Gust, Chem. Soc. Rev. 42 (2013) 755;
(b) A. Kascatan-Nebioglu, M.J. Panzner, C.A. Tessier, C.L. Cannon, W.J. Youngs, Coord. Chem. Rev. 251 (2007) 884.

[3] (a) K.M. Hindi, M.J. Panzner, C.A. Tessier, C.L. Cannon, W.J. Youngs, Chem. Rev. 109 (2009) 3859;
(b) S. Patil, J. Claffey, A. Deally, M. Hogan, B. Gleeson, L.M. Menéndez, H. Müller-Bunz, F. Paradisi, M. Tacke, Eur. J. Inorg. Chem. (2010) 1020.

[4] (a) A.A.D. Tulloch, A.A. Danopoulos, S.M. Cafferkey, S. Kleinhenz, M.B. Hursthouse, R.P. Tooze, Chem. Commun. (2000) 1247;
(b) E. Kluser, A. Neels, M. Albrecht, Chem. Commun. (2006) 4495;
(c) L. Yang, Y. Li, Q. Chen, J. Zhao, C. Cao, Y. Shi, G. Pang, Transition Met. Chem. 38 (2013) 367.

[5] (a) H.V. Huynh, C.H. Yeo, Y.X. Chew, Organometallics 29 (2010) 1479;
(b) H.V. Huynh, Y.X. Chew, Inorg. Chim. Acta 363 (2010) 1979;
(c) H.V. Huynh, Y. Han, R. Jothibasu, J.A. Yang, Organometallics 28 (2009) 5395;
(d) H. Turkmen, R. Can, B. Cetinkaya, Dalton Trans. (2009) 7039;
(e) H.V. Huynh, Y. Han, J.H. Ho, G.K. Tan, Organometallics 25 (2006) 3267;
(f) S.K. Yen, L.L. Koh, H.V. Huynh, A.T.S. Hor, Aust. J. Chem. 62 (2009) 1047.

[6] D. Krishnan, M. Wu, M. Chiang, Y. Li, P.-H. Leung, S.A. Pullarkat, Organometallics (2013), http://dx.doi.org/10.1021/om400110t.

[7] (a) E. Ihara, Y. Ishiguro, N. Yoshida, T. Hiraren, T. Itoh, K. Inoue, Macromolecules 42 (2009) 8608;
(b) E. Ihara, H. Takahashi, M. Akazawa, T. Itoh, K. Inoue, Macromolecules 44 (2011) 3287.

[8] (a) O. Aksin, H. Turkmen, L. Artok, B. Cetinkaya, C. Ni, O. Bueyuekguengoer, E. Oezkal, J. Org. Chem. 691 (2006) 3027;
(b) S. Tandukar, A. Sen, J. Mol. Catal. A: Chem. 268 (2007) 112.

[9] M.G. Clerici, G. Bellussi, U. Romano, J. Catal. 129 (1991) 159.

[10] (a) M. Ghorbanloo, H.H. Monfared, C. Janiak, J. Mol. Catal. A: Chem. 345 (2011) 12;
(b) P. Altmann, M. Cokoja, F.E. Kühn, J. Organomet. Chem. 701 (2012) 51.

[11] N. Mizuno, K. Yamaguchi, K. Kamata, Coord. Chem. Rev. 249 (2005) 1944.

[12] V. Mirkhani, M. Moghadam, S. Tangestaninejad, I. Mohammadpoor-Baltork, E. Shams, N. Rasouli, Appl. Catal. A. Gen. 334 (2008) 106.

[13] E.M. McGarrigle, D.G. Gilheany, Chem. Rev. 105 (2005) 1563.

[14] A.F. Pozharskii, Zh. Obshch. Khim. 34 (1964) 630.

[15] M.J. Frisch, G.W. Trucks, H.B. Schlegel, G.E. Scuseria, M.A. Robb, J.R. Cheeseman, G. Scalmani, V. Barone, B. Mennucci, G.A. Petersson, H. Nakatsuji, M. Caricato, X. Li, H.P. Hratchian, A.F. Izmaylov, J. Bloino, G. Zheng, J.L. Sonnenberg, M. Hada, M. Ehara, K. Toyota, R. Fukuda, J. Hasegawa, M. Ishida, T. Nakajima, Y. Honda, O. Kitao, H. Nakai, T. Vreven, J.A. Montgomery, Jr., J.E. Peralta, F. Ogliaro, M. Bearpark, J.J. Heyd, E. Brothers, K.N. Kudin, V.N. Staroverov, R. Kobayashi, J. Normand, K. Raghavachari, A. Rendell, J.C. Burant, S.S. Iyengar, J. Tomasi, M. Cossi, N. Rega, J.M. Millam, M. Klene, J.E. Knox, J.B. Cross, V. Bakken, C. Adamo, J. Jaramillo, R. Gomperts, R.E. Stratmann, O. Yazyev, A.J. Austin, R. Cammi, C. Pomelli, J.W. Ochterski, R.L. Martin, K. Morokuma, V.G. Zakrzewski, G.A. Voth, P. Salvador, J.J. Dannenberg, S. Dapprich, A.D. Daniels, O. Farkas, J.B. Foresman, J.V. Ortiz, J. Cioslowski, D.J. Fox, Gaussian 09, Revision B.1, Gaussian Inc, Wallingford, CT, 2009.

[16] A.G. Gökçe, S. Gülcemal, M. Aygün, B. Çetinkaya, O. Büyükgüngör, Acta Crystallogr., Sect. C 62 (2006) m535.

[17] D. Meyer, M.A. Taige, A. Zeller, K. Hohlfeld, S. Ahrens, T. Strassner, Organometallics 28 (2009) 2142.

[18] (a) H.M.J. Wang, I.J.B. Lin, Organometallics 17 (1998) 972;
(b) S. Guerret, S. Sole, H. Gornitzka, G. Bertrand, J. Organomet. Chem. 600 (2000) 112;
(c) O. Guerret, S. Sole, H. Gornitzka, M. Teichert, G. Trinquier, G. Bertrand, J. Am. Chem. Soc. 119 (1997) 6668.

[19] (a) W.A. Hermann, V.P.W. Bohn, C.W.K. Gstottmayr, M. Grosche, C.P. Reisinger, T. Weskamp, J. Organomet. Chem. 617–618 (2001) 616;
(b) S. Hohloch, N. Deibel, D. Schweinfurth, W. Frey, B. Sarkar, Eur. J. Inorg. Chem. 12 (2014) 2131.

[20] S. Çekirdek, S. Yaşar, İ. Özdemir, Appl. Organomet. Chem. 28 (2014) 423.

[21] C. Dash, M.M. Shaikh, R.J. Butcher, P. Ghosh, Dalton Trans. 39 (2010) 2515.

[22] (a) W.-H. Yang, C.-S. Lee, S. Pal, Y.-N. Chen, W.-S. Hwang, I.J.B. Lin, J.-C. Wang, J. Organomet. Chem. 693 (2008) 3729;
(b) H.V. Huynh, Y. Han, R. Jothibasu, J.A. Yang, Organometallics 28 (2009) 5395.

[23] (a) A. Weiss, H. Pritzkow, W. Siebert, Angew. Chem., Int. Ed. 39 (2000) 547;
(b) A. Weiss, V. Barba, H. Pritzkow, W. Siebert, J. Organomet. Chem. 680 (2003) 294.

[24] (a) S. Patil, A. Deally, B. Gleeson, H. Müller-Bunz, F. Paradisi, M. Tacke, Appl. Organomet. Chem. 24 (2010) 781;
(b) S. Patil, A. Deally, B. Gleeson, F. Hackenberg, H. Müller-Bunz, F. Paradisi, M. Tacke, Z. Anorg. Allg. Chem. 637 (2011) 386.

[25] S. Patil, A. Deally, B. Gleeson, H. Müller-Bunz, F. Paradisi, M. Tacke, Metallomics 3 (2011) 74.

[26] S.J. Hock, L.-A. Schaper, A. Pöthig, M. Drees, E. Herdtweck, O. Hiltner, W.A. Herrmann, F.E. Kühn, Dalton Trans. 43 (2014) 2259.

[27] R. Sen, D. Saha, S. Koner, Catal. Lett. 142 (2012) 124.

[28] D. Prasetyoko, H. Fansuri, Z. Ramli, S. Endud, H. Nur, Catal. Lett. 128 (2009) 177.

[29] P. Buranaprasertsuk, Y. Tangsakol, W. Chavasiri, Catal. Commun. 8 (2007) 310.